

STRESS ANALYSIS OF EXPONENTIALLY GRADED NA-B₄C AND HCS-MgO PRESSURIZED CYLINDER USING ADOMIAN DECOMPOSITION METHOD

NAPONSKA ANALIZA EKSPONENCIJALNO FUNKCIONALNOG CILINDRA POD PRITISKOM OD NA-B₄C I HCS-MgO PRIMENOM ADOMIAN METODE DEKOMPOZICIJE

Originalni naučni rad / Original scientific paper

Rad primljen / Paper received: 15.07.2024

<https://doi.org/10.69644/ivk-2025-siA-0025>

Adresa autora / Author's address:

¹⁾ Department of Mathematics, School of Chemical Engineering and Physical Science, Lovely Professional University, Phagwara, India, *email: sandeepkumar@gmail.com

²⁾ Symbiosis Institute of Business Management, Symbiosis International (Deemed University), Bangalore, India

³⁾ Department of Mathematics, Pandit Deendayal Energy University, Gandhinagar, India

⁴⁾ United World Institute of Technology, Karnavati University, Gandhinagar, Gujarat, 382422, India

Keywords

- functionally graded material
- cylinder
- Young's modulus
- pressure
- stresses

Abstract

In this paper, elastic stress analysis for functionally graded (FG) pressurized cylinder under steady state condition is done by using Adomian Decomposition Method (ADM). The Young's modulus for the functionally graded material (FGM) is differing exponentially along radial direction, but the Poisson ratio is considered to be invariant. The inner and outer surfaces of the pressurized cylinder are formed of metals and ceramics, respectively. The governing equations including stress-strain relation, strain-displacement and Hooke's law are presented under plane strain conditions. The elastic solutions for radial displacement and stresses are obtained by applying ADM and further obtained results are validated with previously published results with another iterative and numerical technique. For practical understating of the work, two material combinations nickel alloy-boron carbide (NA-B₄C) and high carbon steel-magnesium oxide (HCS-MgO) are considered for numerical interpretations and results are depicted graphically.

INTRODUCTION

In recent years, functionally graded materials (FGMs) have become increasingly well-known as an advanced composite material over traditional composites because of their smooth material property gradation across the material dimension. In 1980, researchers from Japan originally proposed the idea of using FGMs to develop a material that may address the issue of a significant temperature difference between the space shuttle's exterior and interior surfaces. These materials are an inhomogeneous mixture of ceramic and metal that are designed to allow a smooth transition of material properties from one surface to another through the ceramic-reinforced metal matrix. FGMs provide strong material strength under extreme thermomechanical loading conditions and reduced stress concentration at the interface region because of their ability to provide smooth material gradation. In various engineering fields, including

Ključne reči

- funkcionalni kompozitni materijal
- cilindar
- modul elastičnosti
- pritisak
- naponi

Izvod

U radu se izvodi analiza elastičnih napona primenom Adomian metode dekompozicije (ADM) kod funkcionalnog kompozitnog materijala (FGM) cilindra, stacionarno opterećenog. Jungov modul elastičnosti kod FGM materijala se eksponencijalno menja u radijalnom pravcu, a Poasonov koeficijent se smatra invarijantnim. Unutrašnju i spoljašnju površinu cilindra pod pritiskom čine metali i keramike, respektivno. Polazne jednačine uključuju vezu napon-deformacija, deformacija-pomeranje i Hukov zakon u uslovima ravnog stanja deformacija. Elastična rešenja za rajalno pomeranje i napone dobijaju se primenom ADM, a potom dobijeni rezultati se proveravaju shodno ranije objavljenim rezultatima dobijenim drugom iterativnom i numeričkom metodom. Radi praktičnog razumevanja rada, razmatraju se dve kombinacije materijala, legura nikla-karbid bora (NA-B₄C), i visokouglenični čelik-oksidi magnezijuma (VUČ-MgO), za numeričku interpretaciju, a rezultati su predstavljeni i grafički.

aerospace, defence, automotive, civil engineering, electronics, etc., metal matrix composites with ceramic reinforcement are employed as structural materials. Many scientists and engineers with different expertise in science and engineering are collaborating in this era of multidisciplinary study to find new practical uses for functionally graded materials in their respective domains. There has been some discussion of the issues brought up by the mechanical reactions of functionally graded disks. The intricacy of material gradation, geometric profile, mechanical, and thermal loading has led researchers to strive for appropriate analytical solutions in several study publications in order to determine displacement and stresses. When designing an engineering component, the optimal material must be selected to ensure that the component will operate as intended under thermo-mechanical load. To obtain the best material performance possible, it is crucial to research various material combinations composed of composite materials. This is the motiva-

tion for considering two different functionally graded materials in this study. Using the Cauchy Euler iterative technique, Paul and Sahni /1/ examined the stress response of a functionally graded disk with exponentially variable thickness. The three distinct ceramic-metal combinations for the disk have numerical results that the authors have compared. The solutions for displacement and stress fields along radial and circumferential directions have been derived by Paul and Sahni /2/ using Fourier half range series. The authors look at how grading parameter affects a functionally graded cylinder under mechanical load. In order to address the nickel alloy and its thermal properties, Kumaraswamy et al. /3/ have created hybrid metal matrix composition (MMC). The thermal conductivity and coefficient of thermal expansion for the metal matrix composite are analysed throughout a variety of temperatures. Utilising digital image correlation, Kaboglu /4/ offered investigation of the flexural mechanical properties for creatively sandwiched composite structures made of polyethylene terephthalate, balsa wood, and core with the help of four-point bending conditions. According to their research, these three core materials have a number of benefits over one another in terms of abrupt failure, damage tolerance, stiffness, and shear strength. To investigate the impact of forced convection on aluminium alloy 6061, aluminium alloy 6061 MMC as-cast, and aluminium alloy 6061 post-heat treatment conditions, an experiment is conducted /5/. Analysis shows that metal matrix composite surface temperature is higher than that of base metal, indicating that more heat dissipation is being detected.

The Adomian Decomposition Method (ADM) is used by Akinshilo /6/ to analyse the heat transmission in convection fins. In the study, the author examined the profiles of internal heat generation and temperature-dependent conductivity. The author additionally sought at the effects of thermal conductivity, internal heat generation, and thermo-geometric factors on the fin's temperature and heat flow rate intensity. Deka et al. /7/ examined thermoelastic stresses in FG disks and provided an internal heat-generating solution for the conductive-convective-radiative heat equation. For FG isotropic sandwich and laminated composite plates, researchers /8/ presented their investigation of hyperbolic shear deformation theory with five degrees of freedom. The plates are subjected to parabolic transverse shear strains along its thickness profile with zero traction on its top and bottom surfaces. In order to study the free vibrations in functionally graded material rectangular plates with power law from varied profile forms for the volume fraction of material elements in the thickness direction of FGM plates, Hadji et al. /9/ and Hadji /10/ employed a four variable refined plate theory. The paper describes how the side-to-thickness ratio, aspect, and material distribution affect the fundamental frequencies of FGM plates. In order to study free vibrations in creatively graded sandwich plates as well as in laminated composite plates taking into account the stretching and bending effect, several researchers /11-12/ established a novel five variable theory. In conjunction with the Hamiltonian principle, these models apply higher order shear deformation theory to generate equations of motion for the analysis of transverse shear stresses in the absence of a shear correction

factor, while maintaining zero traction on the plate surface. The buckling analysis of isotropic and orthotropic plates under in-plane loads was investigated by Bourada et al. /13/ using higher shear deformation theory with four variables, where integral terms are utilised in the displacement field rather than derivative terms. By taking into account the higher-order distributions of in-plane displacements inside the thickness of the plate, the displacement field is derived. Belifa et al. /14/ used innovative shear deformation theory of higher order to create an exact solution for the bending and dynamic behaviour of FG rectangular plates. In the absence of a shear correction factor, Zoubida et al. /15/ proposed an improved theory for analysing the static and free vibration in FG beams with the necessary constraint of zero traction surface condition and shear stresses ranging in parabolic shape along the thickness direction. With material qualities varying in the thickness direction, the model offers a solution for the functionally graded beam's static and free vibration frequency. In order to analyse the impact of the thickness-to-length ratio and volume fraction index on the fundamental frequencies of FGM plates, Hadji et al. /16/ studied the dynamic behaviour of FG beams. To do this, they introduced a new first-order shear deformation theory, which allowed them to derive the isotropic governing equations for axial and transverse deformations subject to boundary conditions that had simple forms, just like in the case of isotropic plates.

Bouakkaz et al. /17/ extended this study to FG sandwich beams using the theory of hyperbolic shear deformation beam, accounting for higher-order variation of transverse shear strain through the depth of the beam. They also considered varying material volume fraction in power law form and showed how variable volume gradation and thickness to length ratios affected free vibrations in FG sandwich beams. When there are no shear correction factors, the FG sandwich beams are subject to the zero traction boundary conditions on the surfaces. Piezo-thermo-elastic study for thick spherical and cylindrical FG shells made of functionally graded piezoelectric (FGP) materials was presented by Arefi et al. /18-19/. They provided an example of how non-homogeneity characteristics affected the mechanical and electrical components when electrical and thermomechanical loading was applied. Because of the smooth transition of characteristics along the radial direction, FGP materials can be used as an actuator, sensor, or component of a piezo motor in electromechanical systems. The use of FG piezoelectric cylinders as sensors or actuators in electromechanical systems was investigated by Rahimi et al. /20/. They have anticipated the behaviours of piezoelectric structures, especially those subjected to heat loads, by utilizing a novel idea known as the additional energy. Furthermore, a FGP hollow cylinder attached to the rotating devices is employed to detect angular velocity. The results allow predictions to be made about the behaviour of a FGP revolving cylinder under varying angular velocities. Applying a modified version of the successive approximation method along with Adomian's decomposition, Arefi /21/ has examined a non-linear analysis for functionally graded piezoelectric cylinders under mechanical, thermal, and electric loads. Additionally,

they have contrasted the acquired outcomes with the linear analysis for the identical FGP cylinder.

Mohammadi et al. /22/ have studied the two-dimensional thermoelastic response of cylindrical pressure vessels made of functionally graded carbon nanotube-reinforced composite using the shear deformation theory of order three. The properties of the pressure vessels are calculated for different reinforcement patterns using the rule of mixture. They have looked into how a number of significant factors, including the volume proportion of carbon nanotubes and the elasticity-related Pasternak coefficients, affect the behaviour of thermoelectricity. Arefi and Rahimi /23/ have studied the thermo-elastic behaviour of a clamped-clamped axisymmetric functionally graded cylinder under internal pressure. Using first order shear deformation theory (FSDT) and the Hamilton principle, the authors have developed the principle differential equations. Using the shear deformation theory, Arefi et al. /24/ examined a cylindrical shell reinforced with graphene nanoplatelets (GPLs) and subjected to thermomechanical loads. The Halpin-Tsai micromechanical model and rule of mixtures are used to assess the properties of composite materials with uniform symmetric and asymmetric reinforcement distributions for nano-platelet material. Wang et al. /25/ provide an analysis of cementitious material in the form of a variable ratio for the extrusion-based three-dimensional printability of ceramic sand to silica sand replacement. The polyvinyl alcohol coating that covers ceramic sand grains stops shrinkage and tiny cracks from arising from the absorption of water. Through the coordination of the novel attributes with the continuous printing method, the ideal cementitious material is found. Cubic and beam elements are designed and 3D printed with four different types of interior hollow constructions based on the best lightweight combination. The two-dimensional thermoelastic analysis of FG thick-walled cylinders exposed to thermomechanical loading conditions was studied by Arefi et al. /26/ using the Pasternak theory. For the first order, shear deformation theory describes the displacement field. To obtain the system's basic governing differential equations, the energy approach and Euler equations are employed. Arefi et al. /27/ examined the thermal elasticity static problem of cylindrical-shaped containers, designed with FG carbon nanotube reinforced composite and capable of operating under high pressure, using the theory of shear deformation. An internally pressurized FG piezoelectric cylinder was studied for two dimensions using electro-elasticity by Arefi and Rahimi /28/. Arefi and Rahimi /29/ address the main uses of shells, specifically cylindrical shells, as heat exchangers, pressure vessels, reactors, and other nuclear and chemical equipment. Scientists and engineers from the science and engineering departments are working together to investigate novel and cutting-edge practical uses of these cutting-edge materials in their respective domains in this age of integrative research. When developing engineering components, it is crucial to determine the proper design in order to achieve the intended functioning when the component is subjected to mechanical loading. This sets off the primary driving force for our research and the writing of this report. A thick FGM spherical shell with exponential tailoring feature was

subjected to internal and exterior forces, and Nejad et al. /30/ studied its stress response. Using a composite disk /31/ as a comparison, some researchers examined the thermomechanical response of a FGM spinning sandwich disk under thermomagnetic loading. For the analysis of elastic stress in rotating thick annular disks subjected to clamped-free, clamped-clamped, and free-free boundary conditions, Jalali et al. used the finite difference method (FDM) /32/, while Temimi and Ansari /33/ have developed a semi-analytical method for solving nonlinear equations of second-order multipoint boundary value problems. Many researchers investigated the stress distribution and displacement for a thick-walled FGM sphere using the simple iteration technique and the finite element method, and their results are found to be in good agreement with these two methods /34/. Lin /35/ examined the impact of mechanical load on the displacement of a thin-walled FGM annular disk under various pressure boundary conditions. The concept of hypergeometric differential equation was utilised to solve the Navier equation for the stresses. Using the finite element approach, Sahni and Mehta /36/ assessed the effects of mechanical and thermal loading on a sandwich cylinder with a functional grade.

Using ABAQUS® software, Mars et al. /37/ applied the finite element method to analyse the static response of a functionally graded shell. A significant effect of the inhomogeneity constant on stresses and displacement /38/ is detected in the thermomagnetic elastic response of an axisymmetric functionally graded (FG) sphere that follows the power rule for gradation. For the FG spinning disk, Çalioğlu et al. /39/ employed the FORTAN programme to calculate stresses in closed form. The results were then compared by a numerical solution using ANSYS finite element method. Under the conditions of internal and external pressures /40/, the three most popular material combinations are taken into consideration for comparative analysis of stress behaviour in the cases of functionally graded hollow cylinders, spheres, and thin disks. A functionally graded spinning disk with power law-formed hyperbolic and parabolic thickness profiles is described, utilised, and the results obtained are compared with those of a homogenous disk /41-42/ for the assessment of stress distribution under various pressure situations. A functionally graded disk is said to outperform a disk with a homogeneous thickness in this comparison. An asymmetrically loaded hollow FG cylinder is examined, and the impact of the non-homogeneity parameter on the tangential and radial stresses is demonstrated through analytical methods. The obtained outcomes are then juxtaposed with those derived from the shooting method, which takes into account Runge-Kutta fourth-order /43/. Using the Fourier transform method, Delouei et al. /44/ have investigated the effects of two-dimensional thermal conduction along the radial and longitudinal directions on the axisymmetric functionally graded cylinder. Using Tresca's model for the yield criterion /45/, an analytical solution for elastoplastic stresses of the functionally graded rotating disk is obtained. The analytical solution for exponentially graded isotropic functionally grade material subjected to inner and outer pressure has been derived by Tutuncu /46/ using the power series

approach. The impact of different volume fractions on displacement and stresses has been demonstrated by the author. The stress response of rotating annular and solid FGM disks with varying thickness is analysed using the graded finite element method (GFEM) along radial and axial directions. Young's modulus and other material properties are changing along the radial and axial direction by using the power rule /47/. For spherical and cylindrical pressure vessels composed of functionally graded materials, Paul and Sahni /48-49/ have studied two-dimensional mechanical responses. In order to analyse creep and elastic plastic stress for functionally graded thin rotating disks, Sahni and Sharma /50-51/ have done some research. A thin rotating disk's transitional and elastic-plastic stresses have been determined using transition theory by Sharma et al. /52/.

In this study, modulus of elasticity is assumed with non-linear variation in radial direction, but Poisson's ratio is considered to be invariant. Displacements and stresses are investigated in radial direction under steady state and plane strain condition due to internal and external pressures at the surface of the cylinder. Navier equation for the problems is solved by using Adomian Decomposition Method and the obtained results are further compared with previous published results derived by finite element method and Cauchy-Euler iterative methods /53/. For the numerical computation, two functionally graded cylinders made up of NA-B₄C and HCS-MgO are considered, and the results are depicted graphically.

PROBLEM DESCRIPTION

In this study, an axisymmetric thick hollow cylinder, presented in Fig. 1, is considered under a steady-state plane strain condition with inner and outer radii as r_1 and r_2 respectively. Uniform internal pressure P_1 and external pressure P_2 are applied at the inner and outer surfaces of cylinder. Here, Poisson's ratio ν is kept as constant and the modulus of elasticity $Y(r)$ varies along the radial direction and follows exponential law as

$$Y(r) = Y_i e^{k(r-r_1)}, \tag{1}$$

where: $k = \frac{1}{r_2 - r_1} \log\left(\frac{Y(r_2)}{Y(r_1)}\right)$ is material grading parameter and, $Y(r_1) = Y_i$ and $Y(r_2)$ are elastic constants at inner and outer surfaces of the cylinder, respectively.

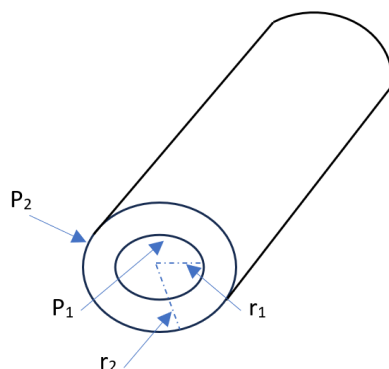


Figure.1 Pressurized graded cylinder with inner and outer radii under internal and external pressures.

The Navier's equation for an axisymmetric functionally graded cylinder can be expressed as /1/,

$$\frac{d\sigma_r}{dr} + \frac{\sigma_r - \sigma_\theta}{r} = 0, \tag{2}$$

where: σ_r and σ_θ are radial and tangential stresses, respectively.

Hooke's law for isotropic material /1/, is considered as,

$$\begin{aligned} \sigma_r &= Y(r) \left(\lambda \frac{du}{dr} + \delta \frac{u}{r} \right), \\ \sigma_\theta &= Y(r) \left(\delta \frac{du}{dr} + \lambda \frac{u}{r} \right), \end{aligned} \tag{3}$$

where: radial displacement u is a function of radius r ; and Lamé's parameters, λ and δ , can be expressed as:

$$\lambda = \frac{1-\nu}{(1+\nu)(1-2\nu)} \quad \text{and} \quad \delta = \frac{\nu}{(1+\nu)(1-2\nu)}. \tag{4}$$

Under the plane strain condition, strain-displacement relation can be expressed as:

$$\epsilon_r = \frac{du}{dr} \quad \text{and} \quad \epsilon_\theta = \frac{u}{r}. \tag{5}$$

Pressure boundary conditions prescribed at inner and outer radii are defined as

$$\sigma_r(r_1) = -P_1 \quad \text{and} \quad \sigma_r(r_2) = -P_2. \tag{6}$$

Using Eqs.(1)-(5), Navier's equation can be expressed in radial displacement as

$$\frac{d^2u}{dr^2} + \frac{1}{r} \frac{du}{dr} - \frac{1}{r^2} u = -k \frac{du}{dr} - \frac{kv}{1-\nu} \frac{u}{r}. \tag{7}$$

ADOMIAN DECOMPOSITION METHOD (ADM)

In this method, we consider differential equations which possess a singularity. To start, consider the singular boundary value problem of order $n + 1$, given by

$$u^{n+1} + \frac{m}{x} u^n + Nu = g(x), \tag{8}$$

subjected to boundary conditions $u(0) = a_0, u'(0) = a_1, u''(0) = a_2, \dots, u^{(n-1)}(0) = a_{n-1}, u(b) = c$, where: N is nonlinear differential operator of order less than n ; $g(x)$ is a given function; and $a_0, a_1, \dots, a_{n-1}, b, c$ are real constants. Consider the following operator L , defined as

$$L(.) = x^{-1} \frac{d^n}{dx^n} x^{n+1-m} \frac{d}{dx} x^{m-n} (.), \tag{9}$$

where: $m \leq n$. Thus, in operator form Eq.(8) becomes

$$Lu = g(x) - Nu. \tag{10}$$

We propose the inverse operator L^{-1} , as defined below

$$L^{-1}(.) = x^{n-m} \int_b^x x^{m-n-1} \int_a^x \dots \int_a^x x(.) dx \dots dx. \tag{11}$$

Applying the inverse operator L^{-1} to both sides of Eq.(8), we have

$$u(x) = \phi(x) + L^{-1}g(x) - L^{-1}Nu, \tag{12}$$

where: $L\phi(x) = 0$.

By applying Adomian decomposition method to Eq.(8), we have the following resulting equation:

$$\sum_{n=0}^{\infty} u_n = \phi(x) + L^{-1}g(x) - L^{-1} \sum_{n=0}^{\infty} A_n, \tag{13}$$

where: A_n are Adomian polynomials that can be evaluated for different forms of nonlinearity. On comparing both sides and using ADM it leads to recursive relation as

$$u_0 = \phi(x) + L^{-1}g(x) = A_0, \quad u_{n+1} = -L^{-1}A_n, \quad (14)$$

where: $n = 0, 1, 2, \dots$

There are many research papers dealing with differential equations that possess singularities. The way to handle such problems is to create a tailored integral operator that overcomes the singular point. The choice of integral operator changes depending on the type of singularity.

IMPLEMENTATION OF ADM TO THE PROBLEM

Equation (7) represents singular ordinary differential equation of order 2, that can be re-written as

$$\frac{d^2u}{dr^2} + \frac{1}{r} \frac{du}{dr} = \frac{u}{r^2} - k \frac{du}{dr} - \frac{kv}{1-\nu} \frac{u}{r}. \quad (15)$$

Differential operator L and inverse operator L^{-1} are defined as

$$L = r^{-1} \frac{d}{dr} \left(r \frac{d}{dr} \right) \quad \text{and} \quad L^{-1}(\cdot) = \int_{r_2}^r r^{-1} \int_{r_1}^r r(\cdot) dr dr. \quad (16)$$

Applying L^{-1} on Eq.(15), we get

$$L^{-1} \left(\frac{d^2u}{dr^2} + \frac{1}{r} \frac{du}{dr} \right) = -L^{-1} \left(k \frac{du}{dr} \right) + L^{-1} \left(\frac{u}{r^2} - \frac{kv}{1-\nu} \frac{u}{r} \right)$$

i.e.,

$$\int_{r_2}^r r^{-1} \int_{r_1}^r \left(\frac{d^2u}{dr^2} + \frac{1}{r} \frac{du}{dr} \right) dr dr = -L^{-1} \left(k \frac{du}{dr} \right) + L^{-1} \left(\frac{u}{r^2} - \frac{kv}{1-\nu} \frac{u}{r} \right).$$

After solving the above equation, we get

$$u(r) = u(r_2) + r_1 u'(r_1) (\log r - \log r_2) - k L^{-1}(u'(r)) + L^{-1} \left(\left(\frac{1}{r^2} - \frac{kv}{1-\nu} \frac{1}{r} \right) u \right), \quad (17)$$

where: $u'(r)$ and $u''(r)$ are first and second derivatives of u with respect to r . Further, by applying the decomposition method on Eq.(17), we get

$$\sum_{n=0}^{\infty} u_n(r) = u(r_2) + r_1 u'(r_1) (\log r - \log r_2) - k L^{-1} \left(\sum_{n=0}^{\infty} u'_n(r) \right) + L^{-1} \left(\left(\frac{1}{r^2} - \frac{kv}{1-\nu} \frac{1}{r} \right) \sum_{n=0}^{\infty} u_n(r) \right). \quad (18)$$

From Eq.(18), recursive equations can be expressed as

$$\begin{aligned} u_0(r) &= u(r_2) + r_1 u'(r_1) (\log r - \log r_2), \\ u_1(r) &= -k L^{-1} u'_0(r) + L^{-1} \left(\left(\frac{1}{r^2} - \frac{kv}{1-\nu} \frac{1}{r} \right) u_0(r) \right), \\ &\vdots, \\ u_{n+1}(r) &= -k L^{-1} u'_n(r) + L^{-1} \left(\left(\frac{1}{r^2} - \frac{kv}{1-\nu} \frac{1}{r} \right) u_n(r) \right), \end{aligned} \quad (19)$$

where: $n = 0, 1, 2, 3, \dots$

Using boundary conditions given by Eq.(6), radial displacement for the HCS-MgO cylinder is presented in Table 2. The result for displacement evaluated up to 5 iterations as

$$u(r) = \sum_{n=0}^5 u_n, \quad (20)$$

and, further by using stress-strain and Hooke's law, radial and tangential stresses are evaluated as

$$\begin{aligned} \sigma_r &= Y(r) \left(\lambda \frac{d}{dr} \left(\sum_{n=0}^5 u_n \right) + \delta \frac{1}{r} \left(\sum_{n=0}^5 u_n \right) \right), \\ \sigma_\theta &= Y(r) \left(\delta \frac{d}{dr} \left(\sum_{n=0}^5 u_n \right) + \lambda \frac{1}{r} \left(\sum_{n=0}^5 u_n \right) \right). \end{aligned} \quad (21)$$

NUMERICAL RESULTS AND DISCUSSION

For the numerical computations, we consider two thick hollow functionally graded pressurized cylinders made up of NA-B₄C and HCS-MgO material combinations with inner radius $r_1 = 0.4$ m and outer radius $r_2 = 0.6$ mm subjected to high internal- low external pressure (50-20 MPa). For the simplicity of the problem constant average Poisson ratio is considered for both materials as shown in Table 1. This table defines material properties for both cylinders.

Table 1. Material properties for the cylinder.

Materials	Young's modulus (inner-outer) GPa	Grading parameter, k	Poisson ratio (inner-outer)	Average Poisson ratio, ν
NA-B ₄ C	205-460	4.04108	0.31-0.17	0.24
HCS-MgO	207.5-317	2.11885	0.295-0.17	0.2325

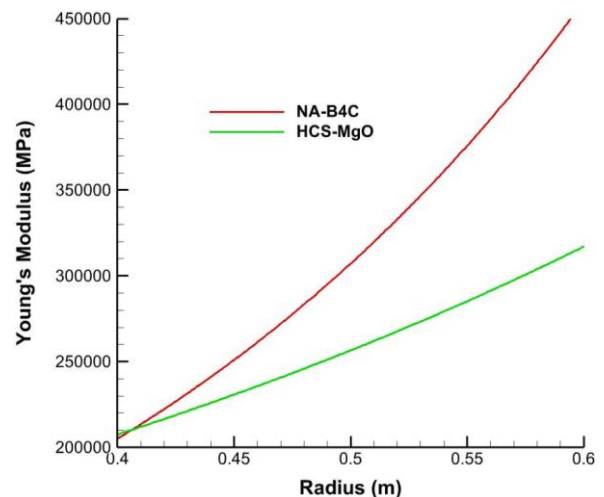


Figure 2. Young's modulus.

Figure 2 shows the exponential variation in Young's modulus along radial direction for both FGM materials. The cylinder made up of NA-B₄C has higher Young's modulus than HCS-MgO cylinder, that shows NA-B₄C cylinder is stiffer than HCS-MgO cylinder. Youngs modulus for both materials are increasing as radius moves from inner to outer surfaces of the cylinder. Tables 2-4 represent radial displacement, radial stress, and tangential stress along 9 radial points equally spaced with a difference of 0.025. These radial points are considered to maintain the simplicity of the table presentation. The comparison of radial displacement of the HCS-MgO cylinder is presented in Table 2. The result for radial displacement is compared with the result obtained by using iterative method and finite element method, /53/.

In this table, it is observed that the relative percentage error in radial displacement between ADM and ITR (iterative) method is very small as compared to the relative percentage error between ADM and FEM (finite element

method). Adomian decomposition method is found to be in good agreement with ITR and FEM methods. Moreover, it required less time of computation, as compared to ITR and FEM for this study. As the radial point moves from inner to outer radii, the relative % error increases for radial displacements. The relative error evaluated by ADM and ITR methods for the radial displacement has minimum error, 0.034 %, at inner surface and maximum error, 0.047 %, at outer surface of HCS-MgO cylinder which is very small as compared to the case where error is evaluated using ADM and FEM.

Table 2. Comparison of radial displacement for HCS-MgO cylinder.

Radius <i>r</i> (m)	Radial displacement <i>u</i>			Relative % error	
	ADM	ITR /53/	FEM /53/	ADM vs. ITR	ADM vs. FEM
0.4	0.0001116640	0.0001117020	0.0001148556	0.034	2.86
0.425	0.0001049200	0.0001049590	0.0001080531	0.037	2.99
0.45	0.0000991417	0.0000991793	0.0001022370	0.038	3.12
0.475	0.0000941643	0.0000942017	0.0000972353	0.040	3.26
0.5	0.0000898584	0.0000898958	0.0000929170	0.042	3.40
0.525	0.0000861194	0.0000861567	0.0000891788	0.043	3.55
0.55	0.0000828619	0.0000828990	0.0000859378	0.045	3.71
0.575	0.0000800155	0.0000800525	0.0000831264	0.046	3.89
0.6	0.0000775223	0.0000775589	0.0000806862	0.047	4.08

In Table 3, relative error is fluctuating along radial points due to the oscillatory behaviour in radial stress. Zero error at the end points and maximum error at *r* = 0.55 can be seen in the last two columns of the table. In this comparison of radial stress, less than 1 % relative error is identified that is remarkable, and further, it can also be reduced more by adding a greater number of iterations in ADM. The comparison of tangential stress in term of relative % error is shown in Table 4. The magnitude of tangential stress by ADM is less than the magnitude of tangential stress obtained by FEM and ITR method. This table shows relative error calculated by ADM and ITR method is less than 0.1 %. Figures 3-5 present the radial displacement and stresses for both NA-B₄C and HCS-MgO pressurized cylinders under the same internal pressure 50 MPa, and external pressure 20 MPa obtained by Adomian decomposition method. The distribution of radial displacement for pressurized cylinders can be seen as of tensile nature in Fig. 3. The magnitude of displacement is falling along the escalating radial points for both materials. Near the internal surface of the cylinder, displacement has higher magnitude as compared to the external surface. It may be due to the higher internal pressure 50 MPa at inner surface and lower external pressure 20 MPa at outer surface of cylindrical body.

Table 3. Comparison of radial stress for HCS-MgO cylinder.

Radius <i>r</i> (m)	Radial stress σ_r			Relative % error	
	ADM	ITR /53/	FEM /53/	ADM vs ITR	ADM vs FEM
0.4	-50	-50	-49.9803	0	0.039
0.425	-44.4222	-44.4208	-44.3984	0.003	0.054
0.45	-39.5844	-39.5811	-39.6315	0.008	0.119
0.475	-35.3440	-35.3391	-35.4967	0.014	0.432
0.5	-31.5916	-31.5859	-31.8013	0.018	0.664
0.525	-28.2420	-28.2363	-28.4735	0.020	0.820
0.55	-25.2278	-25.2232	-25.4099	0.018	0.722
0.575	-22.4950	-22.4924	-22.5819	0.012	0.386
0.6	-20	-20	-19.9933	0	0.034

Table 4. Comparison of tangential stress for HCS-MgO cylinder.

Radius <i>r</i> (m)	Tangential stress σ_θ			Relative % error	
	ADM	ITR /53/	FEM /53/	ADM vs. ITR	ADM vs. FEM
0.4	46.089	46.1103	47.9472	0.046	4.03
0.425	43.6421	43.6634	45.3083	0.049	3.82
0.45	41.7372	41.7588	43.1894	0.052	3.48
0.475	40.2684	40.2903	41.5430	0.054	3.17
0.5	39.1558	39.1781	40.2620	0.057	2.83
0.525	38.3386	38.361	39.3175	0.058	2.55
0.55	37.7699	37.792	38.6407	0.059	2.31
0.575	37.4129	37.4346	38.2151	0.058	2.14
0.6	37.2391	37.2599	37.9774	0.056	1.98

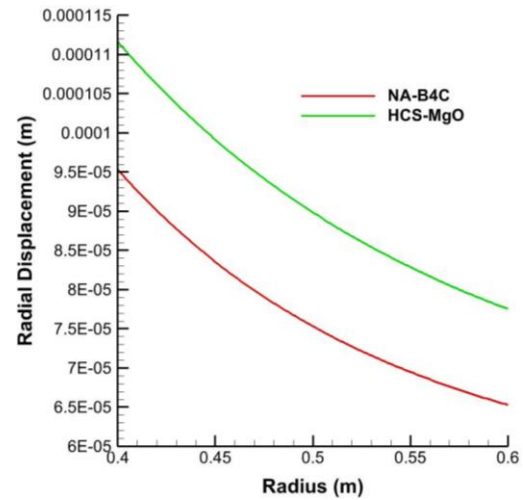


Figure 3. Radial displacement along the radius of cylinder under internal-external pressures, 50-20 MPa.

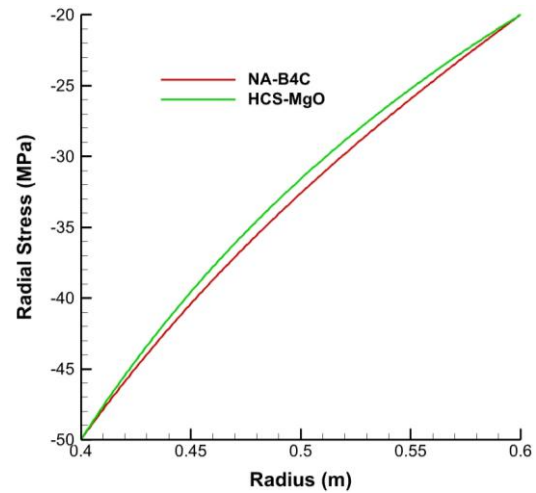


Figure 4. Radial stress along the radius of cylinder under internal-external pressures, 50-20 MPa.

The magnitude of radial displacement in NA-B₄C cylinder is lower than the magnitude of displacement in HCS-MgO cylinder due to higher modulus of elasticity along the inner to outer radii. In Fig. 4, radial stress distributions for both materials are of compressive nature and varying along the increasing radial points from 0.4 to 0.6 m. The radial stress in NA-B₄C cylinder is more compressive than in the HCS-MgO cylinder which means NA-B₄C material provides more elastic strength as compared to the HCS-MgO material to handle the equal amount of pressure. In Fig. 5, it can be observed that tangential stress in tensile form from internal

to external radii of the cylinder is found to be decreasing for HCS-MgO material and increasing for NA-B₄C material under high internal and low external pressure, but for the NA-B₄C cylinder, the magnitude of tangential stress is on the higher side at outer radial points as compared to the HCS-MgO cylinder. This means NA-B₄C provides more withstand capacity than HCS-MgO without failure when it expands under outer pressure. On the other hand, NA-B₄C cylinder has lower magnitude for tangential stress at inner radius as compared to the HCS-MgO cylinder.

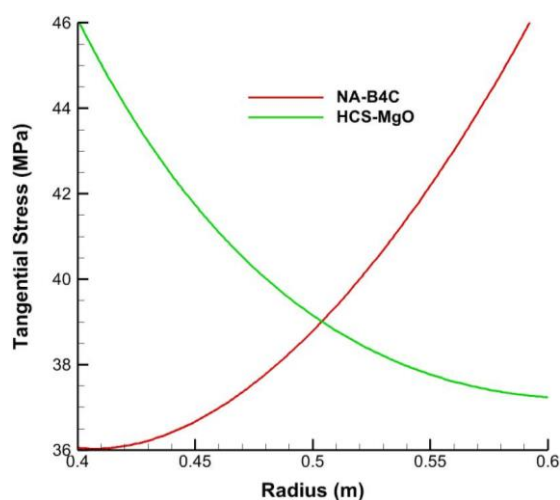


Figure 5. Tangential stress along the radius of cylinder under internal-external pressures, 50-20 MPa.

CONCLUSION

In this paper, the applicability of the Adomian decomposition method (ADM) is discussed by evaluating a semi-analytical solution for stress and displacement for a thick hollow exponentially graded cylinder made up of nickel alloy-boron carbide (NA-B₄C) and high carbon steel-magnesium oxide (HCS-MgO) under high internal and low external pressure. Elastic solutions are derived by using Navier equations under plane strain and steady state condition. The following conclusions are made.

- The elastic response of the disk is strongly dependent on the material combination that is chosen as metal-ceramic pairs. Also, the inhomogeneity parameter has a great impact on stress distribution.
- The result obtained by ADM is found to be in good agreement with the iterative (ITR) and finite element method.
- Relative error comparison shows that ADM is better than iterative technique and the finite element method for this study. Also, the accuracy of Adomian decomposition method can be increased by adding a greater number of iterations.
- In the material comparison, NA-B₄C is found to be good over HCS-MgO as it has more elastic strength to handle the same amount of pressure through the cylinder.
- The derived results can be used in preventing failure in the design of the pressurized cylinder.

REFERENCES

1. Paul, S.K., Sahni, M. (2021), *Stress analysis of functionally graded disk with exponentially varying thickness using iterative*

method, WSEAS Trans. Appl. Theor. Mech. 16: 232-244. doi: 10.37394/232011.2021.16.26

2. Paul, S.K., Sahni, M. (2021), *Two-dimensional stress analysis of a thick hollow cylinder made of functionally graded material subjected to non-axisymmetric loading*, Struct. Integr. Life, Spec. Issue, 2021: S75-S81.
3. Kumaraswamy, J., Kumar, V., Purushotham, G.G., Suresh, R. (2021), *Thermal analysis of nickel alloy/Al₂O₃/TiO₂ hybrid metal matrix composite in automotive engine exhaust valve using FEA method*, J Therm. Eng. 7(3): 415-428. doi: 10.18186/thermal.882965
4. Kaboglu, C. (2017), *The effect of different types of core material on the flexural behavior of sandwich composites for wind turbine blades*, J Therm. Eng. 3(2): 1102-1109. doi: 10.18186/thermal.298608
5. Konchada, P. (2018), *Experimental investigation on Al6061 silver coated copper metal matrix composite circular extended surfaces pre and post heat treatment*, J Therm. Eng. 4(2): 1813-1820. doi: 10.18186/journal-of-thermal-engineering.381820
6. Akinshilo, A. (2019), *Analytical decomposition solutions for heat transfer on straight fins with temperature dependent thermal conductivity and internal heat generation*, J Therm. Eng. 5(1): 76-92. doi: 10.18186/thermal.505489
7. Deka, S., Mallick, A., Behera, P.P., Thamburaja, P. (2021), *Thermal stresses in a functionally graded rotating disk: An approximate closed form solution*, J Therm. Stress. 44(1): 20-50. doi: 10.1080/01495739.2020.1843377
8. Mahi, A., El Abbes, A.B., Tounsi, A. (2015), *A new hyperbolic shear deformation theory for bending and free vibration analysis of isotropic functionally graded, sandwich and laminated composite plates*, Appl. Math. Model. 39(9): 2489-2508. doi: 10.1016/j.apm.2014.10.045
9. Hadji, L., Khelifa, Z., El Abbes, A.B. (2016), *A new higher order shear deformation model for functionally graded beams*, KSCE J Civ. Eng. 20(5): 1835-1841. doi: 10.1007/s12205-015-0252-0
10. Hadji, L. (2017), *Analysis of functionally graded plates using a sinusoidal shear deformation theory*, Smart Struct. Syst. 19(4): 441-448. doi: 10.12989/sss.2017.19.4.441
11. Bennoun, M., Houari, M.S.A., Tounsi, A. (2016), *A novel five-variable refined plate theory for vibration analysis of functionally graded sandwich plates*, Mech. Adv. Mater. Struct. 23(4): 423-431. doi: 10.1080/15376494.2014.984088
12. Bousahla, A.A., Houari, M.S.A., Tounsi, A., El Abbas, A.B. (2014), *A novel higher order shear and normal deformation theory based on neutral surface position for bending analysis of advanced composite plates*, Int. J. Comput. Meth. 11(6): 135-0082. doi: 10.1142/S0219876213500825
13. Bourada, F., Amara, K., Tounsi, A. (2016), *Buckling analysis of isotropic and orthotropic plates using a novel four variable refined plate theory*, Steel Compos. Struct. 21(6): 1287-1306. doi: 10.12989/scs.2016.21.6.1287
14. Bellifa, H., Benrahou, K.H., Hadji, L., et al. (2016), *Bending and free vibration analysis of functionally graded plates using a simple shear deformation theory and the concept the neutral surface position*, J Braz. Soc. Mech. Sci. Eng. 38(1): 265-275. doi: 10.1007/s40430-015-0354-0
15. Zoubida, K., Daouadji, T.H., Hadji, L., et al. (2016), *A new higher order shear deformation model of functionally graded beams based on neutral surface position*, Trans. Ind. Inst. Met. 69(3): 683-691. doi: 10.1007/s12666-015-0540-x
16. Hadji, L., Daouadji, T.H., Amar Meziane, M.A., et al. (2016), *Analysis of functionally graded beam using a new first-order shear deformation theory*, Struct. Eng. Mech. 57(2): 315-325. doi: 10.12989/sem.2016.57.2.315

17. Bouakkaz, K., Hadji, L., Zouatnia, N., El Abbas, A.B. (2016), *An analytical method for free vibration analysis of functionally graded sandwich beams*, Wind Struct. 23(1): 59-73. doi: 10.12989/was.2016.23.1.059
18. Arefi, M., Khoshgoftar, M.J. (2014), *Comprehensive piezo-thermo-elastic analysis of a thick hollow spherical shell*, Smart Struct. Syst. 14(2): 225-246. doi: 10.12989/sss.2014.14.2.225
19. Arefi, M., Rahimi, G.H., Khoshgoftar, M.J. (2012), *Exact solution of a thick walled functionally graded piezoelectric cylinder under mechanical, thermal and electrical loads in the magnetic field*, Smart Struct. Syst. 9(5): 427-439. doi: 10.12989/sss.2012.9.5.427
20. Rahimi, G.H., Arefi, M., Khoshgoftar, M.J. (2011), *Application and analysis of functionally graded piezoelectrical rotating cylinder as mechanical sensor subjected to pressure and thermal loads*, Appl. Math. Mech.-Eng. Ed. 32(8): 997-1008. doi: 10.1007/s10483-011-1475-6
21. Arefi, M. (2013), *Nonlinear thermoelastic analysis of thick-walled functionally graded piezoelectric cylinder*, Acta Mech. 224(11): 2771-2783. doi: 10.1007/s00707-013-0888-0
22. Mohammadi, M., Arefi, M., Dimitri, R., Tornabene, F. (2019), *Higher-order thermo-elastic analysis of FG-CNTRC cylindrical vessels surrounded by a Pasternak foundation*, Nanomater. 9(1): 79. doi: 10.3390/nano9010079
23. Arefi, M., Rahimi, G.H. (2012), *The effect of nonhomogeneity and end supports on the thermo elastic behavior of a clamped-clamped FG cylinder under mechanical and thermal loads*, Int. J Pres. Ves. Pip. 96-97: 30-37. doi: 10.1016/j.ijpvp.2012.05.009
24. Arefi, M., Moghaddam, S.K., Bidgoli, E.M.R., et al. (2021), *Analysis of graphene nanoplatelet reinforced cylindrical shell subjected to thermo-mechanical loads*, Composite Struct. 255: 112924. doi: 10.1016/j.compstruct.2020.112924
25. Wang, L., Jiang, H., Li, Z., Ma, G. (2020), *Mechanical behaviors of 3D printed lightweight concrete structure with hollow section*, Arch. Civil Mech. Eng. 20(1): Art. ID 16. doi: 10.1007/s43452-020-00017-1
26. Arefi, M., Abbasi, A.R., Vaziri Sereshk, M.R. (2016), *Two-dimensional thermoelastic analysis of FG cylindrical shell resting on the Pasternak foundation subjected to mechanical and thermal loads based on FSDT formulation*, J Therm. Stress. 39(5): 554-570. doi: 10.1080/01495739.2016.1158607
27. Arefi, M., Mohammadi, M., Tabatabaiean, A., et al. (2018), *Two-dimensional thermo-elastic analysis of FG-CNTRC cylindrical pressure vessels*, Steel Compos. Struct. 27(4): 525-536. doi: 10.12989/scs.2018.27.4.525
28. Arefi, M., Rahimi, G.H. (2014), *Application of shear deformation theory for two dimensional electro-elastic analysis of a FGP cylinder*, Smart Struct. Syst. 13(1): 1-24. doi: 10.12989/sss.2014.13.1.001
29. Arefi, M., Rahimi, G.H. (2012), *Comprehensive thermoelastic analysis of a functionally graded cylinder with different boundary conditions under internal pressure using first order shear deformation theory*, Mechanika, 18(1): 5-13. doi: 10.5755/j01.mech.18.1.1273
30. Nejad, M.Z., Abedi, M., Lotfian, M.H., Ghannad, M. (2012), *An exact solution for stresses and displacements of pressurized FGM thick-walled spherical shells with exponential-varying properties*, J Mech. Sci. Technol. 26(12): 4081-4087. doi: 10.1007/s12206-012-0908-3
31. Dini, A., Nematollahi, M.A., Hosseini, M. (2021), *Analytical solution for magneto-thermo-elastic responses of an annular functionally graded sandwich disk by considering internal heat generation and convective boundary condition*, J Sandwich Struct. Mater. 23(2): 542-567. doi: 10.1177/1099636219839161
32. Jalali, M.H., Shahriari, B. (2018), *Elastic stress analysis of rotating functionally graded annular disk of variable thickness using finite difference method*, Math. Probl. Eng. 2018: 1871674. doi: 10.1155/2018/1871674
33. Temimi, H., Ansari, A.R. (2011), *A new iterative technique for solving nonlinear second order multi-point boundary value problems*, Appl. Math. Comp. 218(4): 1457-1466. doi: 10.1016/j.amc.2011.06.029
34. Nejad, M.Z., Rastgoo, A., Hadi, A. (2014), *Effect of exponentially-varying properties on displacements and stresses in pressurized functionally graded thick spherical shells with using iterative technique*, J Solid Mech. 6(4): 366-377.
35. Lin, W.-F. (2020), *Elastic analysis for rotating functionally graded annular disk with exponentially-varying profile and properties*, Math. Probl. Eng. 2020: 2165804. doi: 10.1155/2020/2165804
36. Sahni, M., Mehta, P.D. (2020), *Thermo-mechanical analysis of sandwich cylinder with middle FGM and boundary composite layers*, Struct. Integr. Life, 20(3): 313-318.
37. Mars, J., Koubaa, S., Wali, M., Dammak, F. (2017), *Numerical analysis of geometrically non-linear behavior of functionally graded shells*, Lat. Amer. J Solids Struct. 14(11): 1952-1978. doi: 10.1590/1679-78253914
38. Nematollahi, M.A., Dini, A., Hosseini, M. (2019), *Thermo-magnetic analysis of thick-walled spherical pressure vessels made of functionally graded materials*, Appl. Math. Mech. 40(6): 751-766. doi: 10.1007/s10483-019-2489-9
39. Çallioğlu, H., Bektaş, N.B., Sayer, M. (2011), *Stress analysis of functionally graded rotating discs: analytical and numerical solutions*, Acta Mech. Sin. 27(6): 950-955. doi: 10.1007/s10409-011-0499-8
40. Kacar, I. (2020), *Exact elasticity solutions to rotating pressurized axisymmetric vessels made of functionally graded materials (FGM)*, Mater. Sci. Eng. Technol. 51(11): 1481-1492. doi: 10.1002/mawe.202000148
41. Bayat, M., Saleem, M., Sahari, B.B., et al. (2008), *Analysis of functionally graded rotating disks with variable thickness*, Mech. Res. Comm. 35(5): 283-309. doi: 10.1016/j.mechrescom.2008.02.007
42. Bayat, M., Saleem, M., Sahari, B.B., et al. (2009), *Mechanical and thermal stresses in a functionally graded rotating disk with variable thickness due to radially symmetry loads*, Int. J Pres. Ves. Piping, 86(6): 357-372. doi: 10.1016/j.ijpvp.2008.12.006
43. Nkene, E.R.A., Ngueyep, L.L.M., Ndop, J., et al. (2018), *Displacements, strains, and stresses investigations in an inhomogeneous rotating hollow cylinder made of functionally graded materials under an axisymmetric radial loading*, World J Mech. 8(3): 59. doi: 10.4236/wjm.2018.83005
44. Delouei, A.A., Emamian, A., Karimnejad, S., Sajjadi, H. (2019), *A closed-form solution for axisymmetric conduction in a finite functionally graded cylinder*, Int. Comm. Heat Mass Transf. 108: 104280. doi: 10.1016/j.icheatmasstransfer.2019.104280
45. Nejad, M.Z., Rastgoo, A., Hadi, A. (2014), *Exact elasto-plastic analysis of rotating disks made of functionally graded materials*, Int. J Eng. Sci. 85: 47-57. doi: 10.1016/j.ijengsci.2014.07.009
46. Tutuncu, N. (2007), *Stresses in thick-walled FGM cylinders with exponentially-varying properties*, Eng. Struct. 29(9): 2032-2035. doi: 10.1016/j.engstruct.2006.12.003
47. Zafarmand, H., Hassani, B. (2014), *Analysis of two-dimensional functionally graded rotating thick disks with variable thickness*, Acta Mech. 225(2): 453-464. doi: 10.1007/s00707-013-0966-3
48. Paul, S.K., Sahni, M. (2019), *Two-dimensional mechanical stresses for a pressurized cylinder made of functionally graded material*, Struct. Integr. Life, 19(2): 79-85.
49. Paul, S.K., Sahni, M. (2021), *Two-dimensional stress analysis of thick hollow functionally graded sphere under non-axisym-*

- metric mechanical loading*, Int. J. Math. Eng. Manag. Sci. 6(4): 1115-1126. doi: 10.33889/IJMEMS.2021.6.4.066
50. Sharma, S., Sahni, M. (2008), *Creep analysis of thin rotating disc under plane stress with no edge load*, WSEAS Trans. Appl. Theor. Mech. 3(7): 325-338.
51. Sahni, M., Sharma, S. (2017), *Elastic-plastic deformation of a thin rotating solid disk of exponentially varying density*, Res. Eng. Struct. Mater. 3(2): 123-133. doi: 10.17515/resm2016.41me0401
52. Sharma, S., Sahni, M., Kumar, R. (2010), *Elastic plastic analysis of a thin rotating disk of exponentially variable thickness with inclusion*, WSEAS Trans. Math. 9(5): 314-323.
53. Paul, S.K., Mehta, P.D., Sahni, M. (2022), *Numerical simulation of stresses in functionally graded HCS-MgO cylinder using iterative technique and finite element method*, Materials, 15(13): 4537. doi: 10.3390/ma15134537

© 2025 The Author. Structural Integrity and Life, Published by DIVK (The Society for Structural Integrity and Life 'Prof. Dr Stojan Sedmak') (<http://divk.inovacionicentar.rs/ivk/home.html>). This is an open access article distributed under the terms and conditions of the Creative Commons Attribution-NonCommercial-NoDerivatives 4.0 International License